

# VISIBLE TEST ON BUGHOLE GENERATION OF FLUIDITY CONCRETES FOR TUNNEL LINING

ISAMU YOSHITAKE<sup>1</sup>, MASAHIRO HIEDA<sup>1</sup>, KENTA OKAMOTO<sup>2</sup>,  
and TOMOYUKI MAEDA<sup>2</sup>

<sup>1</sup>*Dept of Civil and Environmental Engineering, Yamaguchi University, Ube, Yamaguchi, Japan*

<sup>2</sup>*Penta-Ocean Construction, Tokyo, Japan*

Bughole (surface air-void) is a concern for surface quality though it rarely decreases strength properties of the concrete structure. In particular, sidewall of NATM tunnel lining which generally has negative angle is a significant concern in the bughole problem. To reduce the surface imperfection of concrete, the authors examined the bughole properties and discussed on construction methods in previous investigations. The present study focuses on the relation of bughole generation and concrete viscosity. A visible test of bughole generation was conducted using high and medium fluidity concretes in addition to the conventional concrete. Bughole distribution and properties were analyzed by the image analysis which was developed in our previous study. This paper reports the effect of concrete fluidity on decrease of bugholes on concrete surface. A remarkable observation in the experimental study is that number and area-ratio of bugholes increased with concrete viscosity while large voids can be decreased by using high/medium fluidity concrete.

*Keywords:* Surface air-void, Surface quality of concrete structures, Water-soluble cellulose thickener, WSCT.

## 1 INTRODUCTION

To improve surface quality of concrete structures, bugholes should be reduced as much as possible. Bughole problem is not only aesthetic of concrete, it may influence on maintenance of concrete structures. Smooth surface without bugholes can contribute to easy clean for concrete surface and to check-up of durability such as gas-permeability test.

Numerous construction engineers have tried to decrease the imperfection of the concrete surface. However, we have little effective reduction method of the surface air-voids even now. The author's research group has conducted various experiments to observe bughole generations and to reduce the surface imperfection (Maeda *et al.* 2014, Harada *et al.* 2015, Maeda *et al.* 2016). The previous experimental study focused on bughole problems of conventional concrete in road tunnel constructed by New Austrian Tunnel Method (NATM). The sidewall of NATM tunnel lining which generally has a negative angle is a significant concern in bughole problem.

In Japanese highways, medium fluidity concrete has been often used in NATM tunnels for improvement of concrete-construction. Voids at concrete-casting, a cause of bugholes, can be reduced in case of fluidity concrete. It should be noted that thickener is often used in such fluidity concretes. In such high viscosity concrete, it may be hard to remove surface air-voids under the vibration of the concrete.

The focus of this study is to examine the effect of thickener on concrete bugholes. A laboratory test was conducted to observe bughole generation of the fluidity concrete. The experimental study used a transparent acrylic form to observe concrete voids before/after vibration. The observed bugholes were quantified in an image analysis developed in a previous study (Yoshitake *et al.* 2018). This paper reports bughole distributions and properties based on the image analysis.

## 2 METHODOLOGY

### 2.1 Materials and Concrete Mixtures

The present study used ordinary Portland cement defined in Japanese Industrial Standard (JIS) R5210 for the fluidity concretes. In addition, the study used sea-sand for fine aggregate and crushed sandstone for coarse aggregate. The chemical admixtures used in the study were a poly-carboxylic acid high-range water reducing agent (HRWRA) and a water-soluble cellulose thickener. The materials are given in Table 1.

Table 1. Materials used in the study.

Materials	Symbol	Properties
Cement	C	ordinary Portland cement, density: 3.15 g/cm <sup>3</sup>
Fine aggregate	S	sea sand, density: 2.60 g/cm <sup>3</sup>
Coarse aggregate	G <sub>1</sub>	crushed sandstone, 20-15 mm density: 2.70g/cm <sup>3</sup>
	G <sub>2</sub>	crushed sandstone, 15-5 mm density: 2.70g/cm <sup>3</sup>
Admixture	HRWRA	a poly-carboxylic acid high-range water reducing agent
	WSCT	water-soluble cellulose thickener

Table 2 gives concrete mixtures. The thickeners (WSCT) in the range of 0 to 0.45 % of water were added to the concrete. Fresh properties such as slump-flow and air content are also summarized in Table 2.

Table 2. Mixture proportions and fresh properties.

I.D.	w/cm	W kg/m <sup>3</sup>	C kg/m <sup>3</sup>	S kg/m <sup>3</sup>	G <sub>1</sub> kg/m <sup>3</sup>	G <sub>2</sub> kg/m <sup>3</sup>	HRWRA g/m <sup>3</sup>	WSCT g/m <sup>3</sup>	Air %	Slump Flow cm
T00	0.512	174	340	869	458	458	1.7	0	5.3	45×44
T05	0.512	174	340	869	458	458	2.7	87	3.3	49×43
T10	0.512	174	340	869	458	458	3.4	174	3.4	48×40
T15	0.512	174	340	869	458	458	3.4	261	4.4	47×47
T30	0.512	174	340	869	458	458	5.1	522	4.9	45×43
T45	0.512	174	340	869	458	458	6.8	783	4.9	44×43

### 2.2 Visible Test

To observe bughole generation under vibration, the study used a transparent acrylic form shown in Figure 1. Dimensions of the inner space of the form were 300-mm thickness × 300-mm width × 750-mm height. The 300-mm thickness was based on the design thickness of the lining

concrete of an NATM tunnel. The vibrator used in the present study had a diameter of 28-mm and a frequency of 220–280 Hz. Fresh concrete was cast into the form with an angle of 30 degree and consolidated for 60 seconds using the vibrator. The negative angle form was designed to simulate sidewall of tunnel linings which often appeared bugholes. Front and sides surface conditions of concrete were photographed by using three commercial digital still cameras which have approximately 18 million (5184 × 3456) usable pixels.



Figure 1. Transparent acrylic form and photography condition.



Figure 2. Interface of the image analyzing software.

### 2.3 Image Analysis

Image analyses based on thresholding are conducted to detect and evaluate the bugholes randomly distributed in concrete surface (Liu and Yang 2017, Liu *et al.* 2017). The present study also conducted an image analysis; however, it analyses colored photographs for detection of bugholes. The image analysis can detect invisible bugholes and calculate automatically bughole size. The image analysis is demonstrated in Figure 2. Further details of the image analysis are available in the previous paper (Yoshitake *et al.* 2018).

### 3 RESULTS AND DISCUSSION

#### 3.1 Air-Voids and Bugholes

Air voids before vibrating are frequently observed during general concrete construction. It is well known that the air voids include entrapped air at concrete casting. Vibrators are generally used to remove such air voids in the construction of tunnel lining concrete. To improve concrete quality, medium fluidity concrete (MFC) has been often used in NATM tunnel construction in recent years. Harada *et al.* (2017) performed the image analysis of air-voids of various concretes including a self-consolidating concrete (SCC) and MFC. They also used the transparent acrylic form shown in Figure 1. The purpose of this study is to examine the air-voids of various MFC in addition to the previous investigation (Harada *et al.* 2017).

Figure 3 (a) (b) present surface photographs of conventional concrete and the MFC (T15) tested in this study, respectively. These photos show concrete conditions before vibrating for consolidation. It can be confirmed that MFC has significantly lower air-voids than the conventional concrete tested in the previous study (Harada *et al.* 2017).



(a) conventional concrete (slump:16.5 cm, air:5.5%). (b) MFC (T15) (S.F.: 47 × 47cm, air: 4.4%).

Figure 3. The surface condition of concrete without vibration.

To quantify the air-voids of the tested MFC, the study uses an empirical equation given in Eq. (1) by referring to the previous study (Harada *et al.* 2017).

$$r_a = \frac{S_f \times \sqrt{(S_{sl} + S_{sr})/2}}{V} \times 100 \quad (1)$$

where  $r_a$  is the pseudo-air-void volume ratio (%),  $S$  represents area of air-voids ( $\text{mm}^2$ ) and  $V$  is concrete volume ( $\text{mm}^3$ ). The subscripts  $f$ ,  $sl$ ,  $sr$  represent front, left-side and right-side of concrete specimen, respectively. Each area can be calculated automatically by summing the number of pixels in the photograph.

Bugholes generated under vibration were detected and evaluated by using the image analysis mentioned above. Bugholes of hardened concrete may be slightly different from the bugholes of fresh concrete, however, the differences were negligible. The present study focuses on the bugholes detected in the image analysis of tested fresh concrete (MFC) and quantified the bughole characteristics. To compare the bugholes of each tested concrete (MFC), the study employs the bughole area ratio defined in Eq. (2) as well as previous studies (Harada *et al.* 2015, Maeda *et al.* 2016, Harada *et al.* 2017, Yoshitake *et al.* 2018).

$$r_b = \frac{S_f}{S} \times 100 \quad (2)$$

where  $r_b$  is the bughole area ratio of front concrete surface (%).  $S_f$  and  $S$  are area of bugholes and concrete area for evaluation, respectively.

### 3.2 Image Analysis of Air-Voids

Table 3 summarizes the pseudo air-void volume ratio ( $r_a$ ) obtained from the image analysis. For comparison, the test data reported in the previous investigation (Harada *et al.* 2017) was added to the table. The note is that the ‘‘Conventional’’ in this table means general purpose ready-mixed concretes which include various water-cement ratios (0.42 – 0.70) and designed slump (8, 15, 21 cm). Further information such as mixture proportions are available in the previous study (Harada *et al.* 2017).

Table 3. Pseudo air-void volume ratio ( $r_a$ ) and bughole area ratio ( $r_b$ ).

I.D.	WSCT -g/m <sup>3</sup> -	$r_a$ %	$r_b$ %
T00	0	0.227	0.954
T05	87	1.061	1.082
T10	174	2.342	1.753
T15	261	0.031	1.570
T30	522	0.229	1.521
T45	783	0.335	2.686
MFC <sup>a</sup>	N/A	2.410	1.060
SCC <sup>a</sup>	N/A	0.011	1.330
Conventional <sup>a</sup>	N/A	13.746 – 44.287	0.346 – 1.425

a: previous test data (Harada *et al.* 2017)

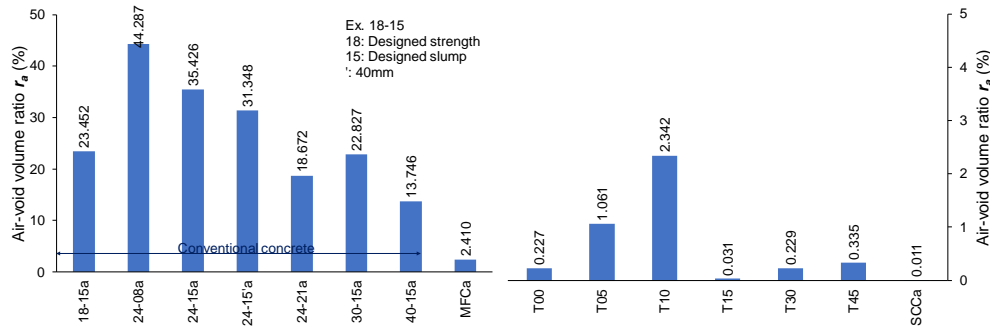


Figure 4. Variation of the pseudo air-void volume ratio ( $r_a$ ).

Figure 4 presents the pseudo air-void volume ratio ( $r_a$ ) varied by addition of the thickener (WSCT). Obvious tendency due to the thickener was not observed in this study while the volume ratios were significantly lower than the ratio of previous MFC. Different from the self-consolidating concrete (SCC), even the medium fluidity concrete (MFC) needs vibration to remove air-voids. The initial condition of such air-void distribution may be due to the casting concrete, so the air-void volume ratios ( $r_a$ ) were not so different by the thickener.

### 3.3 Image Analysis of Bugholes

Figure 5 (a) shows the variation of area-ratio ( $r_b$ ) of bughole having 5 mm or larger diameter. As well, Figure 5 (b) presents the area-ratio ( $r_b$ ) of bughole having 5 mm or smaller diameter.

Noteworthy is that the area-ratio of large bugholes is proportional to the volume of thickener (Figure 5 (a)). Meanwhile, the difference of the area-ratio of small bugholes was small by the thickener as shown in Figure 5 (b).

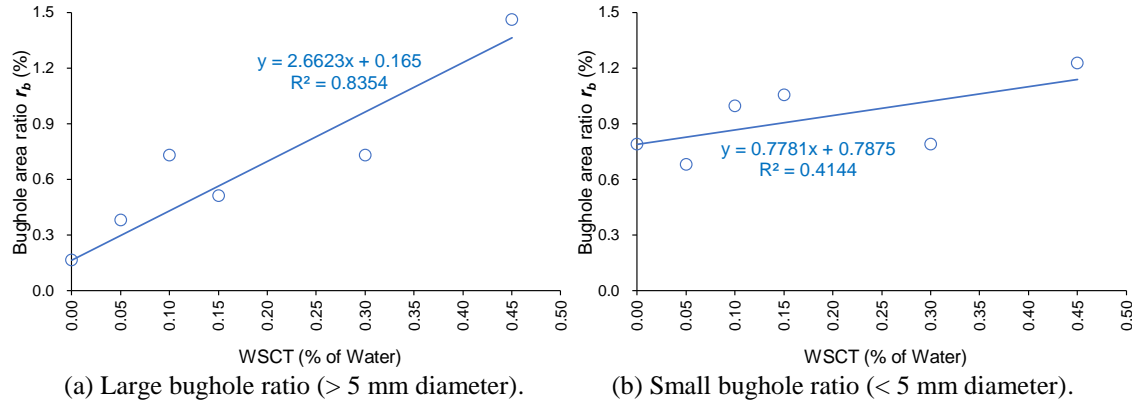


Figure 5. Bughole area ratio ( $r_b$ ) – thickener.

#### 4 CONCLUSIONS

The present study focused on a relation of bughole generation and viscosity of medium fluidity concrete (MFC) including thickener. The visible test was conducted to observe bughole generation during vibration. The conclusions of the study are as follows.

- The air-void volume ratios of MFC using the present thickener were lower than the ratio of previous MFC and conventional concrete.
- The area-ratio of large bugholes (> 5 mm dia.) was proportional to the volume of thickener, while the area-ratio of small bugholes (< 5 mm dia.) was hardly varied by the thickener.

#### References

- Harada S., Maeda T., Hirano M., and Yoshitake I., *Reducing Bug-Holes on Tunnel Lining Concrete by Using Covering Sheets*, Proceedings of ISEC-8, 689-694, Sydney, 2015.
- Harada S., Hieda T., Maeda T., Hirano M., Miyamoto K., and Yoshitake I., Experimental Investigation on Characteristics of Bughole Generation Based on a Visualization Test for Various Concretes (in Japanese), *Journal of the Society of Materials Science, Japan*, 66(8), 582-587, Aug. 2017.
- Liu B., and Yang T., Image Analysis for Detection of Bugholes on Concrete Surface, *Construction and Building Materials*, Elsevier, 137, 432-440, April 2017.
- Liu B., Yang T., and Xie Y., Factors Influencing Bugholes on Concrete Surface Analyzed by Image Processing Technology, *Construction and Building Materials*, Elsevier, 153, 897-907, Oct. 2017.
- Maeda T., Honma H., Hirano M., and Yoshitake I., *Permeability of Tunnel Lining with Air/Water Bubbles on Concrete Surface*, Proceedings of ASEA-SEC-2, 321-325, Bangkok, 2014.
- Maeda T., Harada S., Moriuchi M., and Yoshitake I., *Reevaluation of the Effect of Covering Sheets for Reducing Bugholes on Tunnel Lining Concrete*, Proceedings of EURO-MED-SEC-1, 79-84, Istanbul 2016.
- Yoshitake I., Maeda T., and Hieda M., Image Analysis for the Detection and Quantification of Concrete Bugholes in a Tunnel Lining, *Case Studies in Construction Materials*, Elsevier, 8, 116-130, June 2018.